

THE CRYSTAL STRUCTURES OF YAVAPAIITE,  $\text{KFe}(\text{SO}_4)_2$ ,  
AND GOLDICHITE,  $\text{KFe}(\text{SO}_4)_2 \cdot 4\text{H}_2\text{O}$ <sup>1</sup>EDWARD J. GRAEBER,<sup>2</sup> *Sandia Laboratories, Albuquerque, New Mexico*  
87115 AND ABRAHAM ROSENZWEIG, *Department of Geology*  
*University of New Mexico, Albuquerque, New Mexico 87106.*

## ABSTRACT

Yavapaiite [ $\text{KFe}(\text{SO}_4)_2$ ] crystallizes in space group  $C2/m$  with two formula weights in a unit cell of dimensions  $a=8.152$ ,  $b=5.153$ ,  $c=7.877$  Å,  $\beta=94.90^\circ$ . The structure was solved by a three-dimensional Patterson synthesis and refined by the full-matrix least-squares method to  $R=3.2\%$ . Goldichite [ $\text{KFe}(\text{SO}_4)_2 \cdot 4\text{H}_2\text{O}$ ] in space group  $P2_1/c$  contains four formula weights in a unit cell with  $a=10.387$ ,  $b=10.486$ ,  $c=9.086$  Å,  $\beta=101.68^\circ$ . The structure was solved by hand application of the symbolic addition procedure for phase determination and refined by least squares to  $R=3.3\%$ .

In yavapaiite, ferric sulfate sheets of composition  $n[\text{Fe}(\text{SO}_4)_2]^-$  are linked to coplanar potassium ions; this arrangement accounts for the perfect {001} cleavage. Coordination polyhedra of iron and sulfur are distorted. In goldichite, corrugated sheets of composition  $n[\text{Fe}(\text{SO}_4)_2 \cdot 2\text{H}_2\text{O}]^-$  are linked to potassium and water molecules; this spatial arrangement of the distorted coordination polyhedra accounts for the excellent {100} cleavage. Details of the observed polyhedral distortions are explained by the extended electrostatic valence rule. A plausible hydrogen bonding scheme is presented for goldichite and krausite [ $\text{KFe}(\text{SO}_4)_2 \cdot \text{H}_2\text{O}$ ].

## INTRODUCTION

Although many structures of iron compounds have been reported, only limited data are available for hydrated ferric salts. In general the ferric ion displays octahedral distortions characteristic of the anion type involved; for oxygen coordination to iron the average ferric to oxygen separation is  $\approx 2$  Å although separations vary from 1.91 to 2.24 Å in known structures. Yavapaiite,  $\text{KFe}(\text{SO}_4)_2$ , and goldichite,  $\text{KFe}(\text{SO}_4)_2 \cdot 4\text{H}_2\text{O}$ , are reported here as part of a systematic study of ferric sulfate minerals; krausite,  $\text{KFe}(\text{SO}_4)_2 \cdot \text{H}_2\text{O}$  (Graeber, Morosin, and Rosenzweig, 1965), and coquimbite,  $\text{Fe}_2(\text{SO}_4)_3 \cdot 9\text{H}_2\text{O}$  (Fang and Robinson, 1970), have previously been reported although the anisotropy and hydrogen bonding of coquimbite is presently under investigation.

Yavapaiite was first described by Hutton (1959) on material exposed in the open pit operations of the United Verde Extension Mining Company, Jerome, Arizona. The original description of goldichite was by Rosenzweig and Gross (1955) on crystals from the Dexter No. 7 Mine,

<sup>1</sup> This work was supported by the U.S. Atomic Energy Commission.

<sup>2</sup> A preliminary account of this work was presented at the Eighth International Congress of Crystallography, State University of New York at Stony Brook, August 1969. This material is based on a dissertation submitted in partial fulfillment of the requirements for the doctoral degree at the University of New Mexico.

Calf Mesa, San Rafael Swell, Utah. To our knowledge, these are still the only reported occurrences for each of these minerals.

#### EXPERIMENTAL WORK

Crystals of yavapaiite from the Jerome, Arizona, locality were obtained from Professor Fredrick J. Kuellmer, New Mexico Institute of Mining and Technology, Socorro, New Mexico. The specimen of saccharoidal texture consisted of equidimensional grains averaging 0.2 mm in diameter. The crystals are transparent, short and stubby in form, with their longer dimensions parallel to [010]. Perfect {001} and {100}, and distinct {110} cleavages are reported by Hutton (1959), and the dominance of the two former cleavage directions leads to the development of slender prismatic fragments with roughly rectangular cross sections when crystals are crushed. An attempt was made to obtain spherical crystals (Bond, 1951), but the prominent cleavage caused the grains to fracture before suitable

Table 1. Yavapaiite unit cell data.

	Hutton (1959)	Present Study
$a(\text{\AA})$	8.12	8.152(5)
$b(\text{\AA})$	5.14	5.153(4)
$c(\text{\AA})$	7.82	7.877(5)
$\beta(^{\circ})$	94.40	94.90(7)
$V(\text{\AA}^3)$	325.4	329.7
$a:b:c$ , x-ray	1.580:1:1.521	1.582:1:1.529
, morph.	1.590:1:1.520	---
$D(\text{g.cm}^{-3})$ , calc.	2.92	2.891
, obs.	2.88	---
cell contents		$2[\text{KFe}(\text{SO}_4)_2]$

spheres were obtained. An optically-brilliant single crystal (0.22×0.26×0.30 mm) was mounted according to a method described by Graeber (1961). From  $\text{MoK}\alpha$  precession photographs, the observed systematic absences of  $hkl$  for  $h+k=2n+1$  correspond to space groups  $C2$ ,  $Cm$ , and  $C2/m$ . The zero moment test of Howells, Phillips, and Rogers (1950) employed to resolve this space group ambiguity yielded a distribution of intensities closely resembling a centric distribution. It was concluded that  $C2/m$  is the favored space group. A least-squares refinement of 19 reflections measured at 23°C with  $\text{MoK}\alpha$  radiation gave lattice constants which are compared with Hutton's values in Table 1.

Crystals of goldichite from the type locality at San Rafael Swell, Utah, consisted of small laths elongated parallel to [001] and flattened parallel to the {100} pinacoid. They are colorless, singly terminated, and according to Rosenzweig and Gross (1955), display excellent {100} cleavage. A brilliant crystal of roughly rectangular cross section was cut perpendicular to its long dimension with a diamond-coated wire and subsequently ground into a sphere. After solvent polishing on filter paper with dilute HCl the sphere had a diameter of  $0.34 \pm 0.02$  mm. From  $\text{MoK}\alpha$  precession and Weissenberg photographs the observed systematic absences of  $h0l$  for  $l$  odd and  $0k0$  for  $k$  odd uniquely defined the space group as  $P2_1/c$ . A least-squares refinement of 14 reflections measured at 23°C with

MoK $\alpha$  radiation gave lattice constants which are compared with Rosenzweig and Gross' values in Table 2.

Single crystal intensity data were collected for both minerals on a Picker diffractometer equipped with an E & A full-circle goniometer. Each reflection was integrated by the  $\theta$ ,  $2\theta$  technique using MoK $\alpha$ ; scanning rate was 1°/minute. Background was measured for 20 seconds at each end of the scan with crystal and counter stationary, and was assumed to be a linear function of  $2\theta$  between these points. During data collection, the intensity of a standard reflection was monitored once for every 20 reflections. The intensity fluctuation of the standard reflection was less than 2 percent ( $3\sigma$ ) for both data sets, and it was considered unnecessary to normalize the individual reflection groups. Unique sets of 530 and 1063 reflections were measured for yavapaiite and goldichite respectively; from these sets, 27 and 48 reflections were less than  $3\sigma$  and considered unobserved. Intensities were corrected for

Table 2. Goldichite unit cell data.

	Rosenzweig & Gross (1955)	Present Study
a(Å)	10.45	10.387(6)
b(Å)	10.53	10.486(6)
c(Å)	9.15	9.086(5)
$\beta$ (°)	101.82	101.68(7)
V(Å <sup>3</sup> )	985.5	969.1
a:b:c, x-ray	0.992:1:0.869	0.991:1:0.867
, morph.*	---	---
D(g.cm <sup>-3</sup> ), calc.	2.420	2.461
, obs.	2.43	---
cell contents	4[KFe(SO <sub>4</sub> ) <sub>2</sub> ·4H <sub>2</sub> O]	

\* crystallographic elements unobtainable due to poor quality of reflections from the striated prism zone.

Lorentz and polarization factors to obtain the observed structure amplitudes. No corrections for absorption ( $\mu R_{\text{yavapaiite}}=0.47$  and  $\mu R_{\text{goldichite}}=0.43$ ) or extinction were applied. Atomic scattering factors were interpolated for K<sup>+</sup>, Fe<sup>3+</sup>, S<sup>6+</sup> and O<sup>2-</sup> from Table 3.3.1A of the *International Tables for X-Ray Crystallography*, Vol. III (1962).

#### SOLUTION AND REFINEMENT OF THE STRUCTURES

*Yavapaiite*. A three-dimensional Patterson synthesis revealed six peaks consistent with both (1) calibrated Patterson peak heights,  $H_{ij}$  (Buerger, 1959), and (2) typical separations between sulfur-oxygen and iron-oxygen atom pairs. By placing potassium at 0, 0,  $\frac{1}{2}$ , a structure factor calculation gave an  $R$  value of 0.36. Using weights based upon counting statistics and assigning isotropic thermal parameters, three cycles of full-matrix least squares reduced  $R$  to 0.15. Anisotropic thermal parameters of the form

$$\exp\left(-1/4 \sum_{i=1}^3 \sum_{j=1}^3 B_{ijn} h_i h_j a_i^* a_j^*\right)$$

Table 3. Atomic coordinates and temperature factor coefficients for yavapaiite.

	x	y	z	B <sub>11</sub>	B <sub>22</sub>	B <sub>33</sub>	B <sub>12</sub>	B <sub>13</sub>	B <sub>23</sub>	B <sub>iso</sub>
Fe	0	0	0	0.72	0.36	0.92		-0.07		0.67
K	0	0	½	2.23	1.78	1.05		0.29		1.69
S	0.3701(1)	0	0.2020(1)	0.67	0.31	0.70		0.10		0.56
O(1)	0.2371(3)	0	0.0626(4)	0.75	1.08	1.42		-0.19		1.08
O(2)	0.3128(4)	0	0.3702(4)	1.94	2.29	1.04		0.69		1.76
O(3)	0.4741(3)	0.2325(4)	0.1807(3)	1.51	0.70	1.45	-0.55	-0.41	0.43	1.22

were refined by three cycles of least squares which resulted in a final  $R$  value of 0.032. The final atomic positional parameters with their estimated standard deviations calculated by the method of Cruickshank (1949) and the individual anisotropic temperature factors are listed in Table 3.

*Goldichite.* The goldichite structure was solved by direct methods through the symbolic addition procedure (Karle and Karle, 1966). The data were corrected for vibrational motion and placed on an absolute scale by means of a  $K$  curve thus giving  $F_h^2$ . Statistical averages for the normalized structure factors and the distribution of  $E$  magnitudes favored the centrosymmetric space group. Phases were determined by hand application of the  $\Sigma_2$  expression where the origin was specified by assigning signs to three linearly independent reflections (Hauptman and Karle, 1953). Two other reflections were also specified with letter symbols as shown in Table 4.

From the list of 152 values of  $|E| > 1.5$ , 128 signs were found (31 signs being either + or - and 97 signs in terms of the symbols  $A$  and  $B$ ). Because of the relationships that

Table 4. Initial phase assignments for goldichite.

$h$	$E_h$	$\phi_h$
5 3 $\bar{1}$	2.655	0
2 3 1	2.619	0
6 2 1	2.156	$\pi$
6 7 3	2.955	$a$
3 1 6	2.629	$b$

developed during the application of the symbolic addition procedure, there were strong indications that the symbolic sign of  $A$  was negative. Accordingly,  $E$ -maps were computed for the two combinations - - and - + for  $A$  and  $B$ . The first map ( $A$  -,  $B$  -) contained many spurious peaks, the strongest of which were too closely spaced for iron atoms. The second map ( $A$  -,  $B$  +) clearly resolved the location of ferric ions along with possible sites for sulfate tetrahedra. Coordinates of six prominent peaks (two sulfurs and four oxygens) and the one large iron peak from the map were refined by two cycles of least squares to an  $R$  value of 0.34. Two cycles of difference Fourier syntheses followed by full-matrix least-squares calculations revealed the positions of the remaining nine nonhydrogen atoms, and reduced  $R$  to 0.048. The final  $R$  value with anisotropic temperature factors was 0.033. Atomic positional parameters and individual anisotropic temperature factors are listed in Table 5.

#### DESCRIPTION OF THE STRUCTURES

*Yavapaiite.* A projection of the structure along the  $b$  axis is shown in Figure 1. Potassium ions form a plane separating ferric sulfate sheets of composition  $n[\text{Fe}(\text{SO}_4)_2]^-$ . This arrangement of alternate sheets of negatively charged ferric sulfate and layers of positively charged potassium cations accounts for the perfect  $\{001\}$  cleavage and possibly the tabular habit of yavapaiite. An interesting feature of the polyhedral packing is

Table 5. Atomic coordinates and temperature factor coefficients for goldichite.<sup>a</sup>

	x	y	z	B <sub>11</sub>	B <sub>22</sub>	B <sub>33</sub>	B <sub>12</sub>	B <sub>13</sub>	B <sub>23</sub>	B <sub>iso</sub>
Fe	0.7065(6)	0.1346(6)	0.0935(7)	0.89	0.92	0.84	-0.05	-0.01	-0.02	0.88
K	0.6777(1)	0.7435(1)	0.0351(1)	2.16	2.00	2.40	-0.12	0.89	0.08	2.17
S(1)	0.5253(1)	0.4807(1)	0.2831(1)	0.68	0.74	0.68	-0.13	0.01	-0.03	0.70
S(2)	0.8898(1)	0.3030(1)	0.3557(1)	0.62	0.98	0.88	0.04	0.02	0.10	0.83
O(1)	0.9208(3)	0.4235(3)	0.2907(4)	1.99	1.93	2.67	0.43	0.43	-0.49	2.20
O(2)	0.8639(3)	0.1735(3)	0.0084(4)	0.98	2.96	1.21	0.04	0.05	0.39	1.72
O(3)W	0.8135(3)	-0.0152(3)	0.1957(3)	1.34	1.35	1.57	0.32	0.23	0.26	1.42
O(4)	0.5910(3)	0.5058(3)	0.1598(3)	1.65	1.51	1.31	-0.23	0.34	-0.21	1.49
O(5)	0.6259(3)	0.0214(3)	-0.0728(3)	1.60	1.49	0.95	-0.06	-0.13	-0.25	1.35
O(6)W	0.8376(4)	0.5325(4)	-0.0109(4)	2.64	2.50	1.92	0.28	0.11	0.35	2.35
O(7)	0.5621(3)	0.0938(3)	0.2048(3)	1.31	1.11	1.51	-0.42	0.51	-0.23	1.31
O(8)	0.4500(3)	0.3639(3)	0.2648(4)	1.51	1.37	1.83	0.33	0.07	-0.01	1.57
O(9)W	0.8210(4)	0.6785(4)	0.3321(4)	2.54	2.24	3.12	-0.05	0.83	0.38	2.63
O(10)W	0.6066(3)	0.2910(3)	-0.0027(3)	1.69	1.21	1.21	-0.30	0.16	-0.30	1.37
O(11)	0.9943(3)	0.2114(4)	0.3649(4)	1.46	2.61	2.45	0.86	0.03	-0.41	2.17
O(12)	0.7644(3)	0.2508(3)	0.2651(3)	1.18	1.64	1.34	0.42	0.04	0.66	1.39

O(n)W indicates a water molecule.

<sup>a</sup> Standard errors in parentheses.

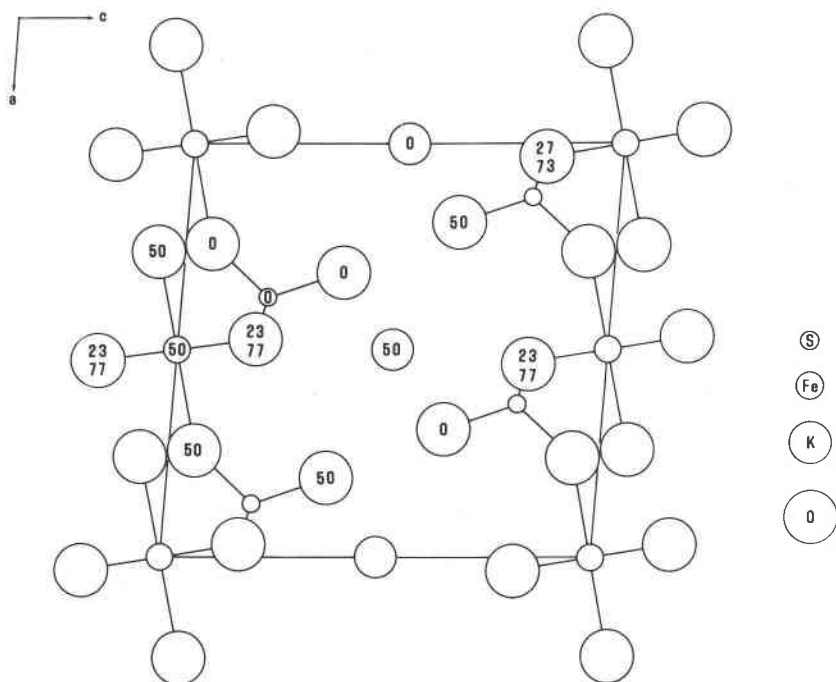


FIG. 1. Projection of the yavapaiite structure along the  $b$  axis. Numbers indicate atom depth below the  $ac$  plane.

the alternating layers of sulfate tetrahedra with ferric-oxygen octahedra when the structure is viewed along  $[\bar{1}10]$ . This arrangement probably accounts for the distinct  $\{110\}$  cleavage found in yavapaiite.

Interatomic separations and angles are given in Table 6. The sulfate tetrahedron is significantly distorted; three sulfate oxygens (average S-O separation of  $1.482 \text{ \AA}$ ) are coordinated to iron, whereas the fourth sulfate oxygen is bonded to potassium. This weaker bond to potassium explains the shorter S-O distance of  $1.442 \text{ \AA}$  and the distortion of the sulfate tetrahedron. Similarly, the deviations of the S-O angles from the ideal may be explained by this bonding. The octahedral coordination about iron is also distorted; four coplanar oxygens have Fe-O separations of  $2.005 \text{ \AA}$  and two oxygens at  $1.954 \text{ \AA}$  complete the octahedral group. Potassium has 10 nearest neighbors at distances ranging from  $2.83$  to  $3.12 \text{ \AA}$ . An idealized geometrical configuration is that of a trigonal antiprism bisected by a square plane. A stereo view of the overall structure in which the coordination polyhedra are emphasized is shown in Figure 2.

The structure of yavapaiite is closely related to krausite (Graeber,

Table 6. Interatomic distances and bond angles for yavapaiite.<sup>a</sup>

Bond	Length	Bond	Length
S - O(2)	1.442(4) Å	O(1) - O(3)	2.393(8) Å [X2]
S - O(1)	1.476(4)	O(1) - O(2)	2.449(8)
S - O(3)	1.485(4) [X2]	O(1) - O(1')	2.773(8) [X2]
		O(1) - O(3')	2.775(8) [X2]
Fe - O(1)	1.954(5) [X2]	O(1) - O(3')	2.824(8) [X2]
Fe - O(3)	2.005(5) [X4]	O(1) - O(3')	3.380(9) [X2]
		O(2) - O(3)	2.393(8) [X2]
K - O(2)	2.827(7) [X2]	O(2) - O(3')	3.324(9) [X2]
K - O(3)	2.860(7) [X4]	O(2) - O(2')	3.497(9) [X2]
K - O(2')	3.122(7) [X4]	O(3) - O(3')	2.396(8)
		O(3) - O(3')	2.757(8)
		O(3) - O(3')	2.913(8)
		O(1) - Fe - O(3')	89.0(3)° [X4]
		O(1') - Fe - O(3)	91.0(3) [X4]
		O(3) - Fe - O(3')	86.8(3) [X2]
		O(3') - Fe - O(3)	93.2(3) [X2]
		O(3) - Fe - O(3)	180.0(4) [X3]
		O(2) - S - O(1)	114.1(3)
		O(2) - S - O(3)	109.7(3) [X2]
		O(1) - S - O(3)	107.8(3) [X2]
		O(3) - S - O(3')	107.5(3)

Atoms labeled prime (') are related by symmetry to the corresponding unprimed atoms.

<sup>a</sup> Standard errors in parentheses

Morosin, and Rosenzweig, 1965). In both minerals the sequence of polyhedral elements is almost identical along the *b*-axis direction which also coincides with the optically slow direction *Z*. In Krausite, however, iron is octahedrally coordinated to five sulfate oxygen atoms and one water molecule.

*Goldichite*. A projection of the structure along the *b* axis is shown in Figure 3. Iron atoms are surrounded by four sulfate-oxygen atoms and two water molecules to form a distorted octahedron. Such octahedra are coordinated to sulfur-oxygen tetrahedra to form sheets of  $n[\text{Fe}(\text{SO}_4)_2 \cdot 2\text{H}_2\text{O}]^-$ . These corrugated sheets of polyhedra roughly parallel the *b* axis and lie predominantly in the (100) plane. Potassium ions have as nearest



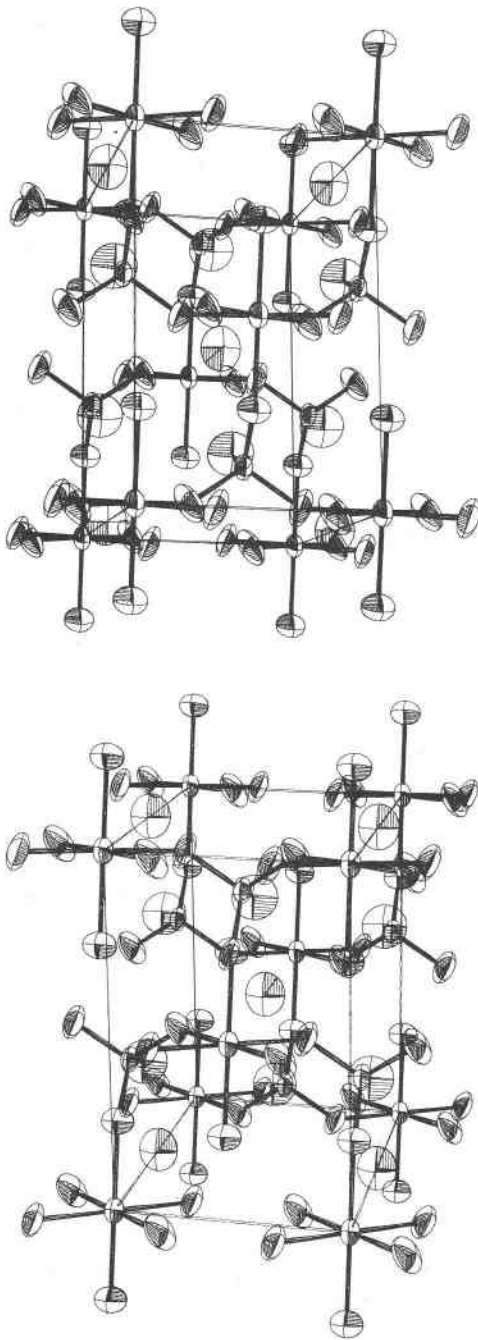


FIG. 2. Stereoscopic illustration of the yavapaiite unit cell. The thermal ellipsoids are scaled to enclose 50 percent probability. Cell origin is at the lower rear left,  $b$  axis vertical and the  $a$  axis horizontal.

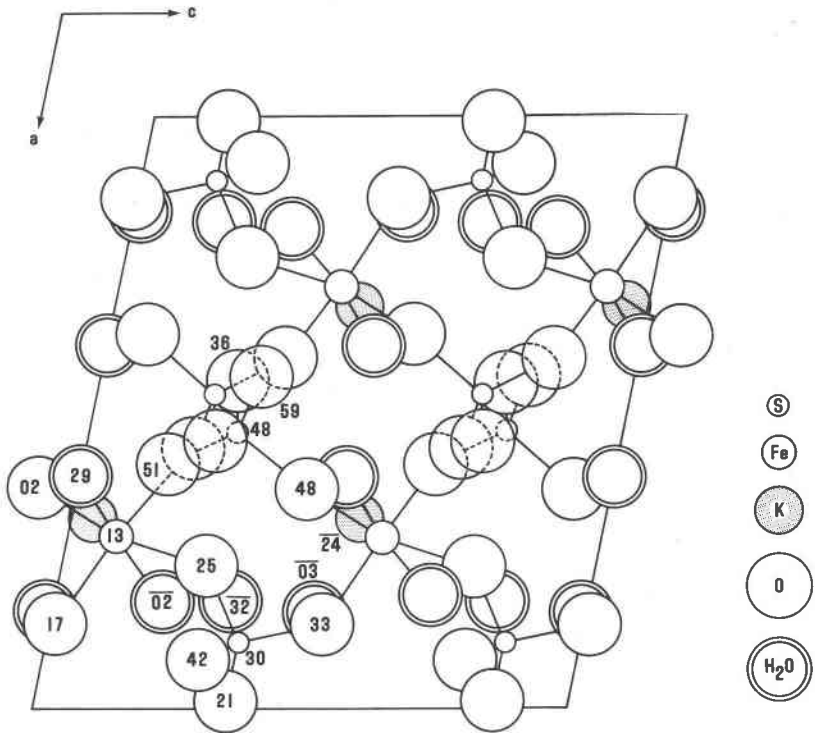


FIG. 3. Projection of the goldichite structure along the  $b$  axis. Numbers indicate atom depth below the  $ac$  plane.

neighbors sulfate oxygen atoms in the sheet and water molecules along  $[001]$  which accounts for the excellent  $\{100\}$  cleavage and possibly the lath-like habit of goldichite.

Interatomic separations and angles are given in Table 7 and Table 8, respectively. Both sulfate tetrahedra are significantly distorted, with each sulfur atom having two longer and two shorter bonds to oxygen atoms. Those sulfate oxygens which have the longer S-O bonds (two from each sulfate group) are shared with iron. Such oxygen atoms serve as the links which form the sheet array. The O-S-O bond angles are close to ideal values although the average linear O-Fe-O angle of  $174.2^\circ$  clearly reflects the observed distortion. Potassium has 11 nearest neighbors at distances ranging from 2.72 to 3.42 Å. Its position in the structure results in bonding together the hydrated ferric sulfate sheets along  $[001]$ . Figure 4 is a stereo view of the structure from which potassium ions and their associ-

Table 7. Interatomic distances for goldichite.<sup>a</sup>

Bond	Length	Bond	Length
S(1) - O(8)	1.444(4)Å	O(1) - O(3') <sub>W</sub>	2.812(8)Å
S(1) - O(4')	1.449(4)	O(1) - O(9') <sub>W</sub>	2.920(8)
S(1) - O(5)	1.501(4)	O(1) - O(6') <sub>W</sub>	2.933(8)
S(1) - O(7')	1.511(4)	O(2) - O(12')	2.379(8)
S(2) - O(11)	1.439(4)	O(2) - O(11')	2.389(8)
S(2) - O(1)	1.458(4)	O(2) - O(3') <sub>W</sub>	2.729(8)
S(2) - O(2')	1.486(4)	O(2) - O(12')	2.854(8)
S(2) - O(12)	1.496(4)	O(2) - O(5')	2.909(8)
		O(2) - O(10') <sub>W</sub>	2.927(8)
Fe - O(5')	1.970(5)	O(3) <sub>W</sub> - O(6) <sub>W</sub>	2.633(8)
Fe - O(12')	1.975(5)	O(3) <sub>W</sub> - O(5')	2.823(8)
Fe - O(2)	1.988(5)	O(3) <sub>W</sub> - O(7')	2.867(8)
Fe - O(7)	2.017(5)	O(3) <sub>W</sub> - O(12)	2.927(8)
Fe - O(3') <sub>W</sub>	2.036(5)	O(4) - O(7)	2.385(8)
Fe - O(10') <sub>W</sub>	2.040(5)	O(4) - O(5')	2.400(8)
		O(4) - O(8')	2.415(8)
K - O(9) <sub>W</sub>	2.720(7)	O(4) - O(10') <sub>W</sub>	2.716(8)
K - O(8')	2.763(7)	O(5) - O(7')	2.401(8)
K - O(6) <sub>W</sub>	2.847(7)	O(5) - O(8)	2.423(8)
K - O(9') <sub>W</sub>	2.887(7)	O(5) - O(7')	2.838(8)
K - O(10) <sub>W</sub>	2.930(7)	O(5) - O(10) <sub>W</sub>	2.914(8)
K - O(4)	2.953(7)	O(6) <sub>W</sub> - O(11')	2.718(8)
K - O(8)	2.999(7)	O(7) - O(8')	2.433(8)
K - O(5)	3.087(7)	O(7) - O(12')	2.638(8)
K - O(3) <sub>W</sub>	3.113(8)	O(7) - O(10) <sub>W</sub>	2.870(8)
K - O(11)	3.360(8)	O(7) - O(10') <sub>W</sub>	2.897(8)
K - O(7)	3.416(8)	O(8) - O(10) <sub>W</sub>	2.890(8)
		O(9) <sub>W</sub> - O(11')	2.897(8)
O(1) - O(2')	2.402(8)	O(10) <sub>W</sub> - O(12)	2.678(8)
O(1) - O(11)	2.403(8)	O(10) <sub>W</sub> - O(12')	2.955(8)
O(1) - O(12)	2.412(8)	O(11) - O(12')	2.412(8)

Atoms labeled prime (') are related by symmetry to the corresponding unprimed atoms.

<sup>a</sup> Standard errors in parentheses.

Table 8. Bond angles for goldichite.<sup>a</sup>

Bond	Angle
O(5') - Fe - O(2)	94.6(3)°
O(5') - Fe - O(7)	90.8(3)
O(5') - Fe - O(3') <sub>W</sub>	89.6(3)
O(5') - Fe - O(10') <sub>W</sub>	93.2(3)
O(12') - Fe - O(2)	92.1(3)
O(12') - Fe - O(7)	82.8(3)
O(12') - Fe - O(3') <sub>W</sub>	93.7(3)
O(12') - Fe - O(10') <sub>W</sub>	83.7(3)
O(2) - Fe - O(3') <sub>W</sub>	85.4(3)
O(2) - Fe - O(10') <sub>W</sub>	93.2(3)
O(7) - Fe - O(3') <sub>W</sub>	90.0(3)
O(7) - Fe - O(10') <sub>W</sub>	91.1(3)
O(5') - Fe - O(12')	172.7(4)
O(2) - Fe - O(7)	172.9(4)
O(3') <sub>W</sub> - Fe - O(10') <sub>W</sub>	177.0(4)
O(8) - S(1) - O(4')	113.2(2)
O(8) - S(1) - O(5)	110.7(2)
O(8) - S(1) - O(7')	110.8(2)
O(4') - S(1) - O(5)	108.9(2)
O(4') - S(1) - O(7')	107.3(2)
O(5) - S(1) - O(7')	105.7(2)
O(11) - S(2) - O(1)	112.1(2)
O(11) - S(2) - O(2')	109.5(2)
O(11) - S(2) - O(12)	110.5(2)
O(1) - S(2) - O(2')	109.3(2)
O(1) - S(2) - O(12)	109.4(2)
O(2') - S(2) - O(12)	105.8(2)

Atoms labeled prime (') are related by symmetry to the corresponding unprimed atoms.

<sup>a</sup> Standard errors in parentheses.

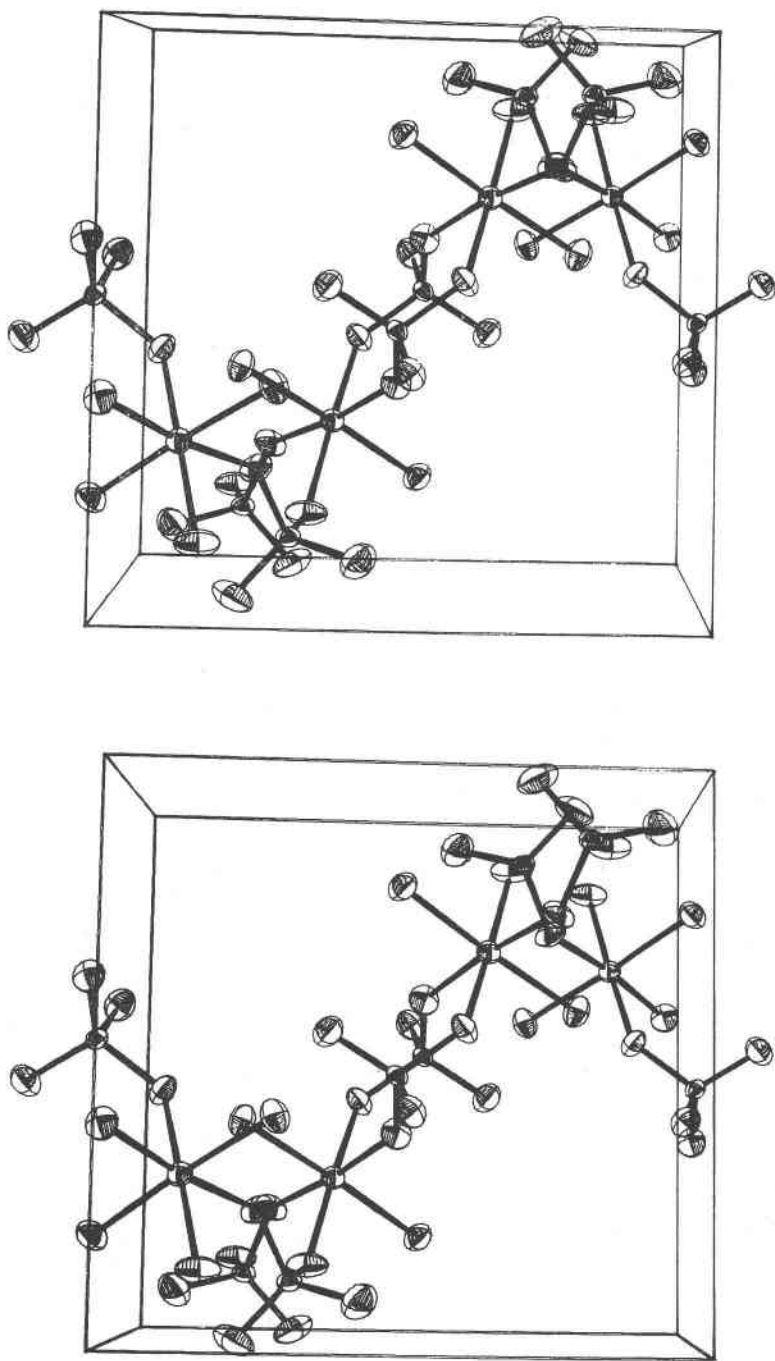


FIG. 4. Stereoscopic illustration of the polyhedral sheets in goldichite unit cell. The thermal ellipsoids are scaled to enclose 50 percent probability. Cell origin is at the lower rear left, *b* axis vertical and the view is parallel to the *c* axis.

Table 9. Electrostatic bond strengths in krausite and goldichite.

krausite	Fe	S	K	H(d)	H(a)	$\zeta$
O(1)		1.5	0.1		0.17	1.77
O(2)		1.5	2x0.1		0.17	1.87
O(3)	0.5	1.5	0.1			2.10
O(4)	0.5	1.5				2.00
O(5)		1.5	3x0.1			1.80
O(6)	0.5	1.5	0.1			2.10
O(7)W	0.5			2x0.83		2.16

goldichite	Fe	S	K	H(d)	H(a)	$\zeta$
O(1)		1.5			3x0.17	2.01
O(2)	0.5	1.5				2.00
O(3)W	0.5		0.09	2x0.83		2.25
O(4)		1.5	0.09		0.17	1.76
O(5)	0.5	1.5	0.09			2.09
O(6)W			0.09	2x0.83	0.17	1.92
O(7)	0.5	1.5	0.09		0.17	2.26
O(8)		1.5	2x0.09			1.68
O(9)W			2x0.09	2x0.83		1.84
O(10)W	0.5		0.09	2x0.83		2.25
O(11)		1.5	0.09			1.59
O(12)	0.5	1.5				2.00

ated water molecules have been deleted in order to clearly show the polyhedral sheets.

#### CHARGE DISTRIBUTION AND HYDROGEN BONDING

It has been shown by Baur (1961) that many of the distortions of coordination polyhedra in ionic or partly ionic compounds can be accounted for by an extension of Pauling's (1960) electrostatic valence rule. The strength ( $s$ ) of an electrostatic bond to each coordinated anion is given by  $s = z/v$  where  $z$  is the electric charge of a cation with coordination number  $v$ . In many stable ionic structures the valence of each anion is nearly equal to the sum of the strengths of the electrostatic bonds to it from adjacent cations; that is,

$$\zeta = \sum_i s_i = \sum_i z_i/v_i$$

Table 10. Bond lengths and  $\zeta$ -values in krausite and goldichite. The values for krausite have been calculated using the parameters published by Graeber, Morosin and Rosenzweig (1965).

Krausite			Goldichite		
	distance	$\zeta$		distance	$\zeta$
Fe-O(4)	1.9 <sup>5</sup> 8 $\overset{\circ}{\text{A}}$	2.00	Fe-O(5)	1.971 $\overset{\circ}{\text{A}}$	2.09
Fe-O(3)	1.974	2.10	Fe-O(12)	1.981	2.00
Fe-O(6)	2.020	2.10	Fe-O(2)	1.987	2.00
Fe-O(7) <sub>W</sub>	<u>2.023</u>	2.16	Fe-O(7)	2.017	2.26
average	1.995		Fe-O(3) <sub>W</sub>	2.037	2.25
			Fe-O(10) <sub>W</sub>	<u>2.037</u>	2.25
			average	2.00 <sup>5</sup>	
S(?) <sub>1</sub> -O(5)	1.445 $\overset{\circ}{\text{A}}$	1.80	S(2)-O(11)	1.438 $\overset{\circ}{\text{A}}$	1.59
S(1)-O(2)	1.448	1.87	S(1)-O(8)	1.448	1.68
S(1)-O(1)	1.455	1.77	S(1)-O(4)	1.451	1.76
S(?) <sub>2</sub> -O(4)	1.481	2.00	S(2)-O(1)	1.459	2.01
S(2)-O(6)	1.494	2.10	S(2)-O(2)	1.488	2.00
S(1)-O(3)	<u>1.497</u>	2.10	S(?) <sub>2</sub> -O(12)	1.491	2.00
average	1.470		S(1)-O(5)	1.500	2.09
			S(1)-O(7)	<u>1.510</u>	2.26
			average	1.473	

and the summation is taken over the cations at the centers of all polyhedra of which the anion forms a corner.

The sums of electrostatic bond strengths presented in Table 9 are calculated assuming that each hydrogen bond contributes 1/6 of one bond strength [column H(a)] to the acceptor atom. This was found to be a reasonable assumption in a number of salt hydrates studied by Baur (1962). The remaining 5/6 of the bond strength is counted towards the sum of the bond strength of the donor atom of the hydrogen bond [column H(d)]. The resulting  $\zeta$ -values are listed in Table 10 together with the bond lengths. It can be seen that generally the bonds involving oxygen atoms which are oversaturated (have a high  $\zeta$ -value) are longer than the average bond length for this polyhedron, while oxygen atoms which are undersaturated form shorter bonds to the cations.

The agreement between observed and calculated bond lengths (Table 11) is of the same magnitude as observed by Baur (1970) from regression analyses of known structures. The hydrogen bond distances in krausite and goldichite range from 2.63 to 2.99 Å (hydrogen donor to oxygen

Table 11. Comparison of observed and calculated bond lengths for krausite and goldichite.

krausite				goldichite			
	$\Delta\zeta$	$d_{\text{obs}}$	$d_{\text{calc}}$		$\Delta\zeta$	$d_{\text{obs}}$	$d_{\text{calc}}$
a) Bond lengths in the Fe-coordination. Calculated lengths based on $d(\text{Fe-O})=(2.011+0.22\Delta\zeta)$ .				Calculated lengths based on $d(\text{Fe-O})=(2.011+0.22\Delta\zeta)$ .			
Fe-O(3)	0.01	1.974	2.013	Fe-O(2)	-0.14	1.987	1.980
Fe-O(3)	0.01	1.974	2.013	Fe-O(3)W	0.11	2.037	2.035
Fe-O(4)	-0.09	1.958	1.991	Fe-O(5)	-0.05	1.971	2.000
Fe-O(6)	0.01	2.020	2.013	Fe-O(7)	0.12	2.017	2.037
Fe-O(6)	0.01	2.020	2.013	Fe-O(10)W	0.11	2.037	2.035
Fe-O(7)W	0.07	2.028	2.026	Fe-O(12)	-0.14	1.981	1.980
b) Bond lengths in the sulfate group. Calculated lengths based on $d(\text{S-O})=(1.473+0.128\Delta\zeta)$ .				Calculated lengths based on $d(\text{S-O})=(1.473+0.128\Delta\zeta)$ .			
S(1)-O(1)	-0.19	1.455	1.449	S(1)-O(4)	-0.19	1.451	1.449
S(1)-O(2)	-0.09	1.448	1.461	S(1)-O(5)	0.14	1.500	1.491
S(1)-O(3)	0.14	1.497	1.491	S(1)-O(7)	0.31	1.510	1.514
S(1)-O(3)	0.14	1.497	1.491	S(1)-O(8)	-0.27	1.448	1.438
S(2)-O(4)	0.00	1.481	1.473	S(2)-O(1)	0.11	1.459	1.487
S(2)-O(5)	-0.20	1.445	1.447	S(2)-O(2)	0.10	1.488	1.486
S(2)-O(6)	0.10	1.494	1.486	S(2)-O(11)	-0.31	1.438	1.433
S(2)-O(6)	0.10	1.494	1.486	S(2)-O(12)	0.10	1.491	1.486
c) Hydrogen bond lengths. Calculated lengths based on $d(\text{O-H}---\text{O})=(2.85-0.38\Delta\zeta)$ .				Calculated lengths based on $d(\text{O-H}---\text{O})=(2.85-0.38\Delta\zeta)$ .			
[case I]				[case I]			
O(7)W-O(1)	0.40	2.83	2.70	O(3)W-O(1)	0.24	2.81	2.76
O(7)W-O(2)	0.30	2.99	2.74	O(3)W-O(6)	0.33	2.63	2.72
[case II]				[case II]			
O(7)W-O(1)	0.23	2.83	2.76	O(6)W-O(1)	-0.09	2.93	2.88
O(7)W-O(1)	0.23	2.83	2.76	O(9)W-O(1)	-0.17	2.92	2.91
				O(10)W-O(4)	0.49	2.72	2.66
				O(10)W-O(7)	-0.01	2.87	2.85

acceptor length). In krausite the hydrogen-bond geometry is satisfied by both the vector in the mirror plane [case I] and the hydrogen-hydrogen vector normal to the mirror plane [case II]. Because of the hydrogen-bond length comparison between observed and calculated distances, case II looks preferable (Baur, personal communication).

## ACKNOWLEDGEMENTS

The authors wish to acknowledge gratefully the kindness of Professor C. Osborne Hutton for his donation of material that formed the basis of the yavapaiite study and to Mr. R. C. Patrick for his assistance in the laboratory in many ways. We wish to thank Dr. B. Morosin from Sandia Laboratories and Drs. D. T. Cromer, A. C. Larson, and R. B. Roof from the Los Alamos Scientific Laboratory for their assistance in crystallographic computa-



tions Copies of Table 12 and Table 13 listing observed and calculated structure factors for yavapaiite and goldichite respectively have been deposited with the American Society for Information Science, The National Auxiliary Publication Service.<sup>1</sup>

## REFERENCES

- BAUR, W. H. (1961) Verzerrte Koordinationspolyeder in heteropolaren Kristallstrukturen und die elektrostatische Valenzregel von Pauling. *Naturwiss.* **48**, 549–550.
- (1962) Zur Kristallchemie der Salzhydrate. Die Kristallstrukturen von  $\text{MgSO}_4$  (Leonhardtite) and  $\text{MgSO}_4 \cdot 4\text{H}_2\text{O}$  (Rozenite). *Acta Crystallogr.* **15**, 815–826.
- (1970) Bond length variation and distorted coordination polyhedra in inorganic crystals. *Trans. Amer. Crystallogr. Assoc.* **6**, (in press).
- BOND, W. L. (1951) Making small spheres. *Rev. Sci. Instr.* **22**, 344–345.
- BUERGER, M. J. (1959) *Vector Space*. New York, John Wiley and Sons, Inc.
- CRUICKSHANK, D. W. J. (1949) The accuracy of electron density maps in x-ray analysis with special reference to dibenzyl. *Acta Crystallogr.* **2**, 65–82.
- FANG, J. H., AND ROBINSON, P. E. (1970) Crystal structures and mineral chemistry of hydrated ferric sulfates. I. The crystal structure of coquimbite. *Amer. Mineral.* **55**, 1534–1540.
- GRAEBER, E. J. (1961) A method for mounting single crystal spheres. *Norelco Rep.*, **8**, 93.
- , MOROSIN, B., AND ROSENZWEIG, A. (1965) The crystal structure of krausite,  $\text{KFe}(\text{SO}_4)_2 \cdot \text{H}_2\text{O}$ . *Amer. Mineral.* **50**, 1929–1936.
- HAUPTMAN, H., AND KARLE, J. (1953) Solution of the phase problem. The centrosymmetric crystal. *Amer. Crystallogr. Ass. Monogr.* **3**.
- HOWELLS, E. R., PHILLIPS, D. C., AND ROGERS, D. (1950). The probability distribution of x-ray intensities. II. Experimental investigation and the x-ray detection of centers of symmetry. *Acta Crystallogr.* **3**, 210–214.
- HUTTON, C. O. (1959) Yavapaiite, an anhydrous potassium ferric sulfate from Jerome, Arizona. *Amer. Mineral.*, **44**, 1105–1114.
- KARLE, J., AND KARLE, I. L. (1966) The symbolic addition procedure for phase determination for centrosymmetric and noncentrosymmetric crystals. *Acta Crystallogr.* **21**, 849–859.
- MACGILLAVRY, C. H., REICK, G. D., AND LONSDALE, K. (1962) *International Tables for X-ray Crystallography*. **3**, Birmingham, England, The Kynoch Press.
- PAULING, L. (1960) *The Nature of the Chemical Bond*. New York, Cornell University Press.
- ROSENZWEIG, A., AND GROSS, E. B. (1955) Goldichite, a new hydrous potassium ferric sulfate from the San Rafael Swell, Utah. *Amer. Mineral.* **40**, 469–480.

*Manuscript received, January 19, 1971; accepted for publication, March 22, 1971.*

<sup>1</sup> Order NAPS Document No. 01520 from National Auxiliary Publications Service of the A.S.I.S., c/o CCM Information Corporation, 866 Third Avenue, New York, N.Y. 10022; remitting \$2.00 for microfiche or \$5.00 for photocopies, in advance payable to CCMIC-NAPS.